

Stress and strain analysis of functionally graded plates with circular cutout

Vikash Singh Dhiraj¹, Nandit Jadvani¹ and Kanak Kalita^{*1,2}

¹Department of Mechanical Engineering, MPSTME, SVKM's NMIMS Shirpur Campus, Dhule, Maharashtra 425405, India.

²Department of Aerospace Engineering & Applied Mechanics, Indian Institute of Engineering Science and Technology, Shibpur, Howrah, West Bengal 711103, India

(Received July 14, 2016, Revised August 30, 2016, Accepted August 31, 2016)

Abstract. Stress concentration is an interesting and essential field of study, as it is the prime cause of failure of structural parts under static load. In the current paper, stress and strain concentration factors in unidirectional functionally graded (UDFGM) plate with central circular cutout are predicted by carrying out a finite element study on ANSYS APDL platform. The present study aims to bridge the lacuna in the understandings of stress analysis in perforated functionally graded plates. It is found that the material variation parameter is an important criterion while designing a perforated UDFGM plate. By selecting a proper material variation parameter and direction of material gradation, the stress and strain concentrations can be significantly reduced.

Keywords: FGM; stress concentration; FEM simulation; circular cut-out; perforated plate

1. Introduction

Since the beginning of the century, there has been immense use of composite materials in various forms such as plates and shells. It has expanded considerably to present day in fields of automotive, construction, aerospace, energy, electronics, chemical engineering, optical materials and biomedical engineering. The composite materials have noteworthy advantages over traditional materials. In conventional multilayer structures, layered composite materials are being used to improve the performance (mechanical, thermal, acoustic etc.) of the structure. The major drawback is stress concentrations at the interfaces due to the change of mechanical and thermal properties. Constant efforts are being made to reduce this stress concentration, and it has bore the concept of Functionally Graded Materials (FGM). The key advantage of FGM is that it overcomes the internal boundary which exists in composites thus preventing the interfacial stress concentration. The initial FGMs were designed to serve as thermal barriers (Yamanouchi and Koizumi 1991). Due to the abrupt changes in the material properties of the laminated composite structures in the transverse direction and subsequently, possibility of local failure occurrence, functionally graded

*Corresponding author, E-mail: kanakkalita02@gmail.com

materials are being used as alternative in some applications. Today, there have been more and more numerous modern engineering applications of FGM, like the spacecraft, rocket engine casings and packaging materials in the microelectronics industry, biomaterials (dental implants) and others (Watari 1997) (Oonishi *et al.* 1994). Many researchers have shown considerable interest in calculating the stress concentration factor (SCF) in perforated FGM plates (Saini and Kushwaha 2014) (Sburlati 2013) (Enab, Stress concentration analysis in functionally graded plates with elliptic holes under biaxial loadings 2014). Stress concentrations around cutouts have great practical importance because they are normally the root cause of failures. Majority of the studies performed for the SCF have treated isotropic, orthotropic or composite plates.

Shen and Noda (Shen and Noda 2007) presented a postbuckling analysis for a functionally graded cylindrical shell with piezoelectric actuators subjected to hydrostatic pressure combined with electric loads in thermal environments. Dag *et al.* (Dag *et al.* 2008) studied the mixed-mode stress intensity factors for an embedded crack in an orthotropic FGM coating. Zhang *et al.* (Zhang *et al.* 2008) conducted the cohesive modeling of dynamic crack growth in homogeneous and functionally graded materials. Shokrolahi-Zadeh and Shodja (Shokrolahi-Zadeh and Shodja 2008) used the concepts of the homogenization, together with spectral consistency conditions and Eshelby-Fourier tensor, to develop the spectral equivalent inclusion method for the study of inhomogeneities with coatings made of functionally graded material. Kim and Amit (Kim and Amit 2008) proposed a generalized interaction integral method for the evaluation of the T-stress in orthotropic functionally graded materials under thermal loading. Zhong and Cheng (Zhong and Cheng 2008) analyzed the crack problem in a functionally graded strip with arbitrary distributed material properties. Shao *et al.* (Shao *et al.* 2008) studied the non-axisymmetric thermal stress in functionally graded hollow cylinders. Li and Lee (Li and Lee 2008) made the fracture analysis of a weak-discontinuous interface in a symmetrical functionally graded composite strip loaded by anti-plane impact. Singh *et al.* (Singh *et al.* 2008) studied the vibration of a solid sphere or shell of functionally graded materials. Wang *et al.* (Wang *et al.* 2005) analyzed the thermal shock strengths of a plate of a functionally graded material when the plate is suddenly exposed to an environmental medium of different temperature. Ding and Li (Ding and Li 2008) dealt with the anti-plane problem of periodic interface cracks in a functionally graded coating-substrate structure.

Based on the literature survey, it can be concluded that limited researches have been conducted to analyze the stress concentration in a functionally graded plate with central cutout. Moreover, almost all the available literature available depicts that the static analysis of FGM plates with cutouts have been carried out only for x-FGM or y-FGM. To the best of authors' knowledge there is no comprehensive work available on stress and strain concentration factors for FGM plates varying radially and angularly. The present paper, aims to study the effect of material variation on stress and strain concentration in unidirectional perforated functionally graded plate.

2. Materials and methods

2.1 Geometry and loading

SCF is the ratio of maximum stress in the cutout periphery to the nominal stress. In accordance with Yang *et al.* (Yang *et al.* 2008) stress concentration factor (K_σ) and strain concentration factor (K_ϵ) are defined as,

$$K_{\sigma} = \frac{\sigma_{max}}{\sigma_{net}} \tag{1}$$

Where, σ_{max} is the maximum stress in the cutout periphery. σ_{net} is the nominal stress and is defined as,

$$\sigma_{net} = \frac{\sigma_x W}{W - D/2} \tag{2}$$

$$K_{\epsilon} = \frac{\epsilon_{max}}{\epsilon_{net}} \tag{3}$$

$$\epsilon_{net} = \frac{\sigma_x W}{E(W - D/2)} \tag{4}$$

Here, W and H, are width and depth of the quarter plate. D is the diameter of the central cutout. σ_x is the applied stress in X-direction. E is the average Young's modulus of the UDFGM plate.

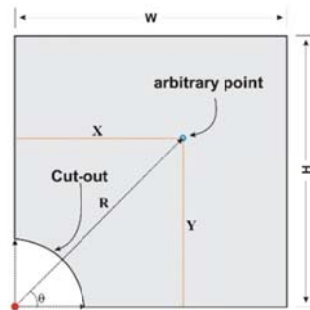
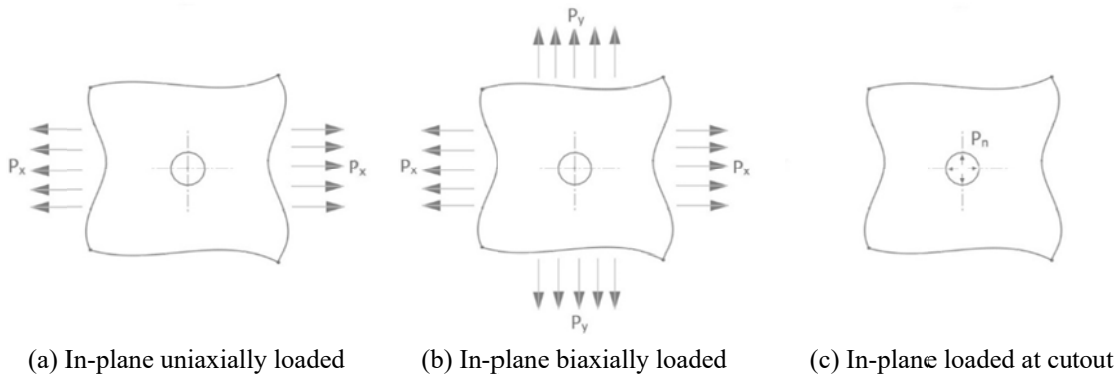


Fig. 1 Quarter plate model of the UDFGM



(a) In-plane uniaxially loaded (b) In-plane biaxially loaded (c) In-plane loaded at cutout

Fig. 2 Various load conditions of the UDFGM plate

The geometric configuration of the perforated infinite FGM plate along with the dimensions considered in the study is shown Fig. 1. Cartesian coordinate system is used with origin located at the center of the central cutout. In this study, $W=100\text{mm}$, $H=100\text{mm}$, $D=20\text{mm}$, $\sigma_x=10\text{Mpa}$ are considered.

Three different load conditions are studied in this paper namely uniaxial uniform pressure load (Fig. 2(a)) and biaxial uniform pressure load (Fig. 2(b)) and in-plane normal load on the cutout periphery (Fig. 2(c)). Also while simulating the biaxial load condition both like and unlike loads are treated i.e. in both $\sigma_x = \sigma_y$ and $\sigma_x = -\sigma_y$ cases are studied.

2.2 Finite element model of UDFGM plate

Commercial finite element software package- ANSYS v14.5 (academic version) has been used in this study to carry out the simulations. The ANSYS parametric design language (APDL) has been used by author(s) (Kalita, Shinde & Thomas, Non-dimensional Stress Analysis of an Orthotropic Plate 2015) (Kalita & Halder, Static Analysis of transversely loaded isotropic and orthotropic plates with central cutout 2014) (Kumar, Agrawal, Ghadai & Kalita 2016) in past to accurately deal with stress study problems. A 2D model of the plate was modelled using isoparametric quadrilateral Plane 183 elements. Plane 183 element has 8 nodes-4 corner and 4 mid nodes with 2 translational degrees of freedom in the nodal X- and Y-directions. The developed models ensure that sufficient control can be maintained over the mesh.

Since the plate is symmetrical in nature, only one quadrant of the plate is modelled and meshed. Mapped meshing is used to get finer mesh near the discontinuity. This finer mesh near the cutout is well equipped in capturing the SCF in this region. The boundary conditions of the quarter model were imposed by constraining the x-displacement (u_x) at $X=0$ and the y-displacement (u_y) at $Y=0$ to account for the planes of symmetry of the full model.

ANSYS does not contain any specified module to incorporate functional grading of material properties. A number of researchers in their work have carried out step wise distribution of material properties instead of continuous variation in property (Enab, Stress concentration analysis in functionally graded plates with elliptic holes under biaxial loadings 2014). This is because the manufacturing technologies of FGM are still in nascent stage and world is yet to see a perfect continuously graded FGM. Real life FGM show step wise material variation. In this work, the FE model is divided into a number of layers and material property is assigned to individual layers in incremental manner. The logic behind doing so is that by assuming a large number a layers and varying the material properties incrementally a real curve of unidirectional functionally graded material can be obtained.

Let's consider a UDFGM plate made of two materials – *Material 1*: Pure titanium ($E=107\text{ GPa}$, $\nu=0.34$) and *Material 2*: Titanium monobromide ($E=375\text{ GPa}$, $\nu=0.14$). Across the X-direction variation in volume fraction is given as (Nemat-Alla, 2003) (Enab, A comparative study of the performance of metallic and FGM tibia tray components in total knee replacement joints, 2012),

$$V_1 = \left(\frac{x}{W}\right)^m$$

$$V_2 = (1 - V_1)$$

Where, suffix 1 and 2 denote material 1 and 2 respectively, W represents width of plate and x is

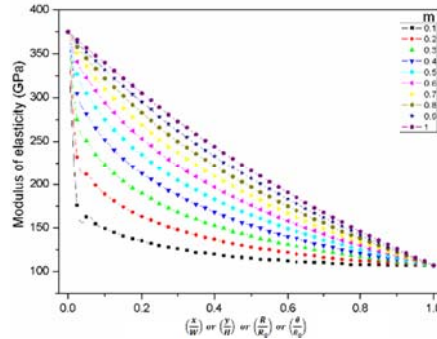


Fig. 3 Variation of modulus of elasticity with respect to geometric position within the perforated plate

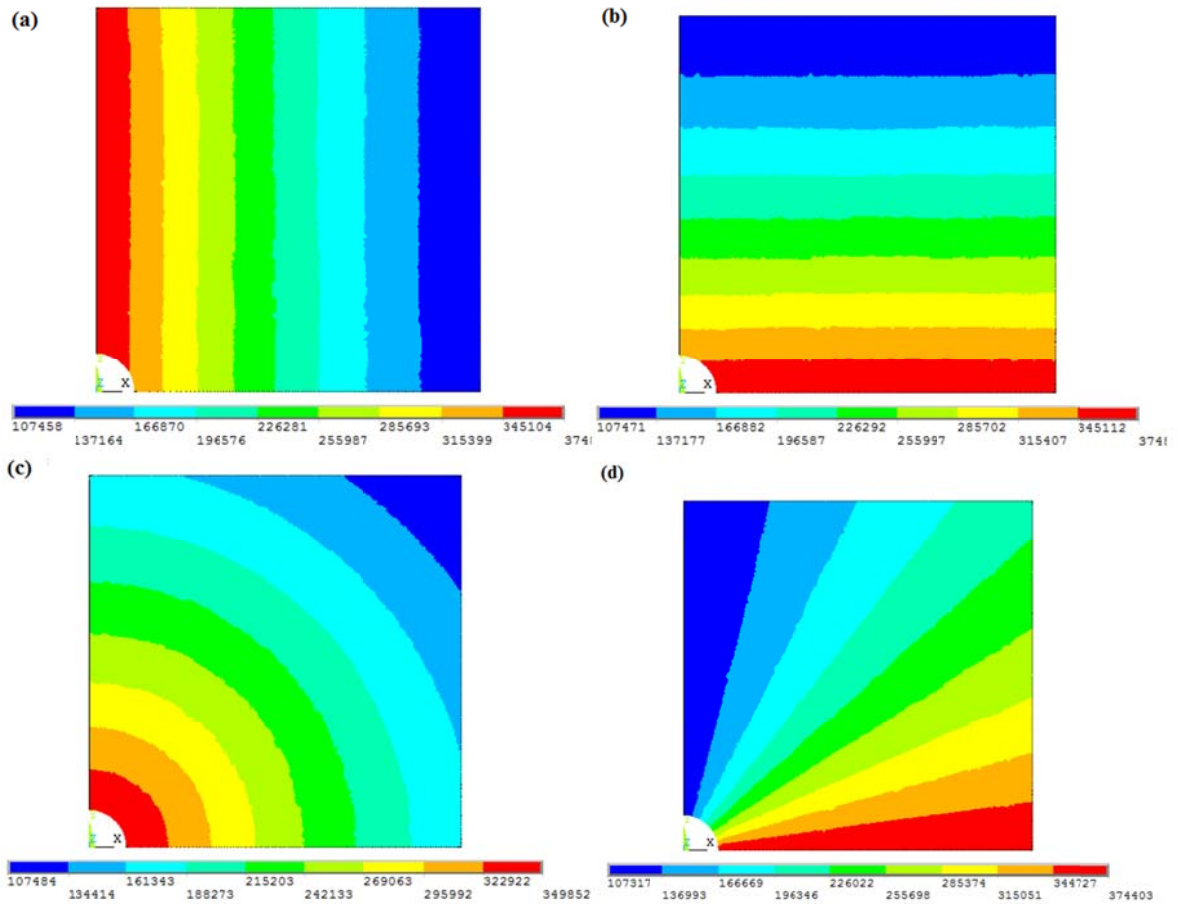


Fig. 4 Modulus of elasticity 2D contours for unidirectional FGM variations ($m=1.0$) in (a) X-direction (b) Y-direction (c) radial direction (d) angular direction

the horizontal position of any point within the FGM plate (Fig. 1). The composition variation of material 1 and 2 in the FGM plate is controlled by the parameter m . When $m < 1$, the FGM plate has material 1 rich composition and for material 2 rich compositions, $m > 1$. At $m = 1$, the variation of

material 1 and 2 composition is linear. The porosity p of the FGM may be represented for horizontal distribution model by

$$p = A \left(\frac{x}{W} \right)^n \left[1 - \left(\frac{x}{W} \right)^z \right]$$

Where

$$0 \leq A \leq \frac{\{(n+z)/n\}^n}{1 - \{(n+z)/n\}^n}$$

A, n and z are arbitrary parameters that control the porosity and in accordance with (Enab, Stress concentration analysis in functionally graded plates with elliptic holes under biaxial loadings 2014) taken as 0.1, 1 and 1 respectively.

$$E = \frac{E_0(1-p)}{1 + \frac{p(5+8\nu)(37-8\nu)}{8(1+\nu)(23+8\nu)}}$$

Where,

$$E_0 = E_2 \left[\frac{E_2 + (E_1 - E_2)V_1^{\frac{2}{3}}}{E_2 + (E_1 - E_2)(V_1^{\frac{2}{3}} - V_1)} \right]$$

$$\nu = \nu_1 V_1 + \nu_2 V_2$$

Here E_0 is the elastic modulus at zero porosity, E_1 , ν_1 and E_2 , ν_2 are the Young's modulus and Poisson's ratio for *Material 1* and *Material 2* respectively.

Similarly the unidirectional variation in Y-, radial and angular direction can be obtained by replacing the $\left(\frac{x}{W} \right)$ in above equations by,

- $\left(\frac{y}{H} \right)$ for y-FGM.
- $\left(\frac{R}{R_0} \right)$ for r-FGM where, $R = \sqrt{x^2 + y^2}$, $R_0 = \sqrt{W^2 + H^2}$
- $\left(\frac{\theta}{\theta_0} \right)$ for θ -FGM where, $\theta = \tan^{-1} \left(\frac{y}{x} \right)$, $\theta_0 = 90^\circ$

The variation in material properties along the layers is controlled by variation of parameter m as formulated above. In actual manufacturing process the parameter m controls the compositions of constituent materials with respect to geometric position. It is worth mentioning here that in this particular study four different types of unidirectional FGM variations are studied- along X-direction, along Y-direction, along radial direction and angular variation. To study the effect of composition variation parameter on the SCF, m is considered from 0.1-1.0 with incremental steps of 0.1. Fig. 3 shows the variation of modulus of elasticity with respect to geometric position within the perforated plate. As seen from the Fig. 3, at m=1 the variation in Young's modulus is linear with larger Young's modulus material near the cutout and minimum Young's modulus at the outer edge. Fig. 4 shows an example (at m=1) of how the modulus of elasticity variation contour plots would look like. The four images show the variation of modulus of elasticity in X-, Y-, radial- and angular direction respectively.

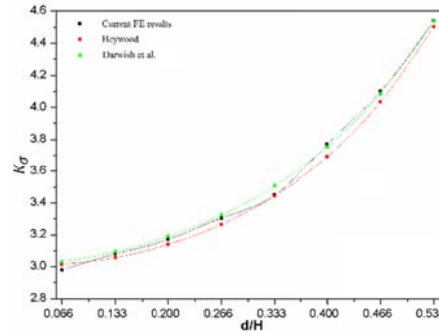


Fig. 5 Comparison between current FE results and literature

3. Validation of finite element model

Since the present analysis is based on finite element models, the validation of the developed models are extremely essential. Therefore, to validate the accuracy of the current results, certain cases in literature are independently reproduced and compared. An isotropic plate of the dimensions $H=100\text{mm}$, $W=100\text{mm}$ and $\sigma_x=10\text{Mpa}$ is considered. The results of the current FE model are compared with the equations presented by Heywood (Young & Budynas 2002) and by Darwish *et al.* (Darwish, Gharaibeh, & Tashtoush 2012). Heywood proposed the following relation for calculation of SCF in a plate with central cutout under uniaxial loading,

$$K_{\sigma} = \frac{2 + \left(1 - \frac{d}{H}\right)^3}{\left(1 - \frac{d}{H}\right)}$$

Where, d is the diameter of the hole and H is plate height.

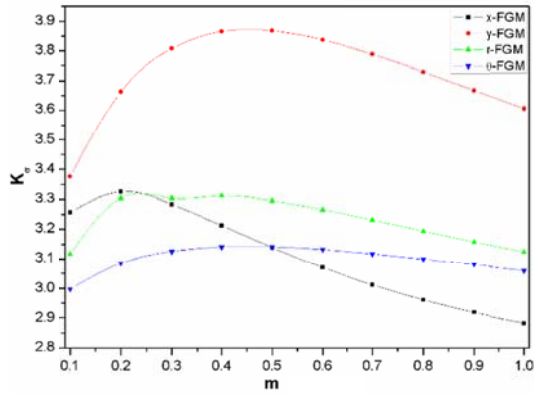
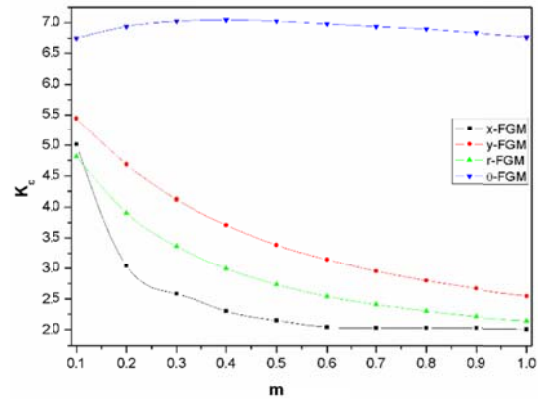
Darwish *et al.* (Darwish, Gharaibeh, & Tashtoush 2012) has introduced an accurate and modified equation,

$$K_{\sigma} = 3 + \frac{\left(\frac{d}{H}\right)^{1.4}}{1 - \left(\frac{d}{H}\right)^{0.5}}$$

As shown in Fig. 5, the current results at different diameter-to-width ratios (d/H) are in excellent agreement with the values computed from Heywood's equation. Also for all d/H ratios the current results are more accurate than Heywood's as they are more close to SCF predicted by Darwish *et al.* Thus, it can be concluded that the current FE models are capable of accurate predictions.

4. Results and discussion

4.1 Uniaxial loading

Fig. 6 Influence of m on K_σ under uniaxial loadingFig. 7 Influence of m on K_ϵ under uniaxial loading

As discussed earlier the material composition parameter (m) is responsible for variation of elastic constants (E and ν) across the plate dimensions. It is called unidirectional FGM because in each case the elastic constants are varied in one particular direction. The stress concentration factor, K_σ for UDFGM plate under tensile load at different values of m is shown in Fig. 6. It is seen that least K_σ is in case of x-FGM. This can be accounted due to the fact that the plate is tensile loaded uniaxially in x -direction i.e. in the same direction of material gradation. But when the y-FGM is similarly tensile loaded uniaxially in x -direction, the material gradation being in perpendicular direction to the applied load has negligible effect on K_σ reduction. Similarly, a θ -FGM is more effective in reducing SCF as compared to an r-FGM when tensile loaded uniaxially.

Fig. 7 shows the variation of strain concentration factor, K_ϵ with respect to material composition constant. The θ -FGM will yield most when loaded uniaxially in x -direction and hence the strain concentration factor is maximum. A close look at Fig. 4(d) will reveal that the material varies un-symmetrically across the loading edge, whereas as in Fig 4(b) the variation in material properties across the loaded edge is uniform in y-FGM. Thus in y-FGM when m approaches unity it means that the material variation tends to be linear. So the Young's modulus varies more uniformly across the loading edge when $m=1$ (linear distribution) as compared to $m=0.1$ (parabolic distribution). Hence K_ϵ in y-FGM, r-FGM and x-FGM decreases monotonically as m approaches unity. The least K_ϵ is recorded for x-FGM because at the loading edge there is no variation in material properties (Fig. 4a).

4.2 Biaxial loading

Fig. 8 depicts the variation of K_σ with respect to m in a biaxially loaded UDFGM. It is observed that K_σ trend lines for x-FGM and y-FGM coincides. The underlying reason is that both the loading condition and geometry are somewhat symmetrical in nature in these two cases. The K_σ in these cases are maximum due to the reason that one of the two loads of biaxial condition is parallel to the direction of material gradation and the other load is perpendicular. It is already seen in the uniaxial loading conditions that when applied load is in same direction as material gradation K_σ is least whereas when load is applied perpendicular to direction of material gradation maximum K_σ will occur. This is perhaps due to the fact that despite our attempts to vary the

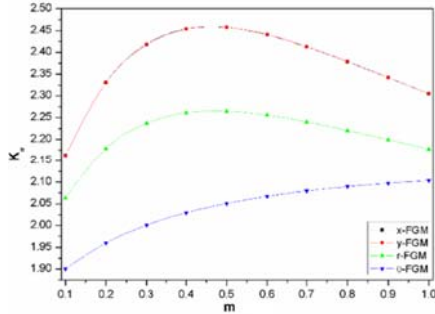


Fig. 8 Influence of m on K_σ under biaxial loading

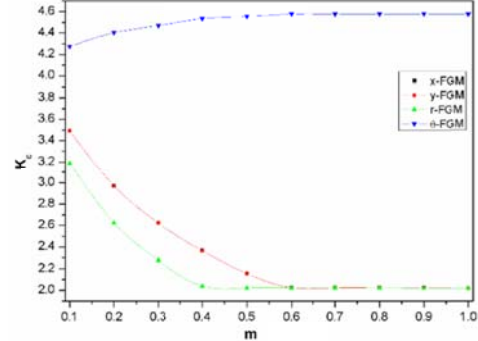


Fig. 9 Influence of m on K_ϵ under biaxial loading

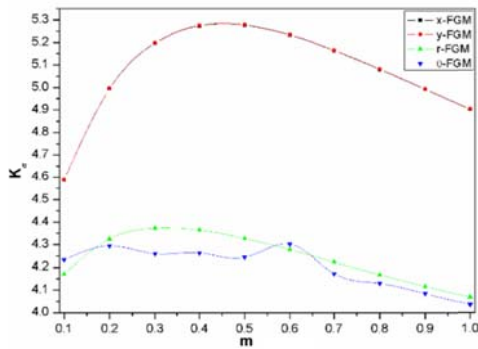


Fig. 10 Influence of m on K_σ under biaxial loading ($\sigma_x = -\sigma_y$)

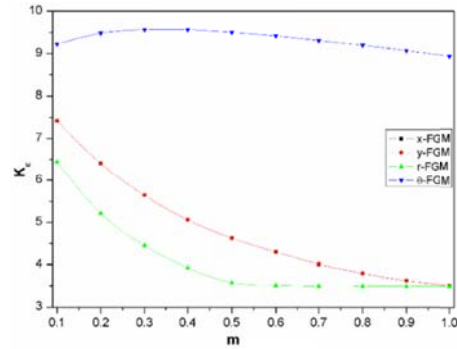


Fig. 11 Influence of m on K_ϵ under biaxial loading ($\sigma_x = -\sigma_y$)

material linearly, in reality this can be considered as a step-wise variation. For instance if a linear variation is made up of small incremental steps and if we sufficiently zoom out, the variation will look like a straight line. So, these interfaces where material property varies are possible sites of stress concentration. Hence when load is applied perpendicular to direction of material gradation significant stresses are generated at these interfaces. It can be also observed that K_σ is minimum in θ -FGM. Observation of Fig. 4(d) highlights that the probable reason is that gradation of material is at both the loading edges.

Fig. 9 shows the variation of K_ϵ with respect to m. It can be observed that maximum strain concentration occurs in θ -FGM. Since the biaxial load is acting on both the edges of symmetrical square plate with hole, in combination with material grading over the plate edges, it is found to be maximum. It can be inferred from Fig. 4(c) that due to radial gradation, the material is varying although the directions, it is relatively divided into small graded parts. The combined effect of biaxial loading and fragmentation of material at both the loading edges, results in minimum K_ϵ in r-FGM.

The biaxial load condition with unlike loads i.e. $\sigma_x = -\sigma_y$ is also treated here. Fig. 10 which shows variation of K_σ with respect to m is somewhat similar to Fig. 8. However as expected K_σ at any given m for biaxially loaded case $\sigma_x = -\sigma_y$ when compared with $\sigma_x = \sigma_y$ is always higher. It can be observed that K_σ is maximum for x-FGM and y-FGM and least for θ -FGM. As explained earlier this is due to the fact that one of the two loads of biaxial condition is parallel to

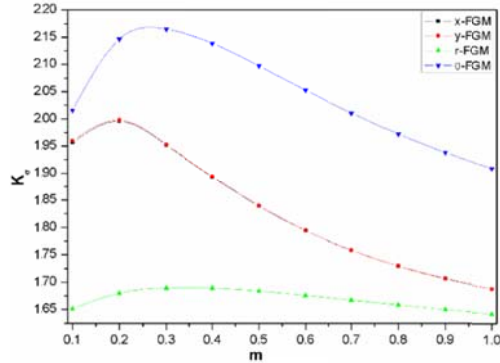


Fig. 12 Influence of m on K_{σ} under loading at cutout edge

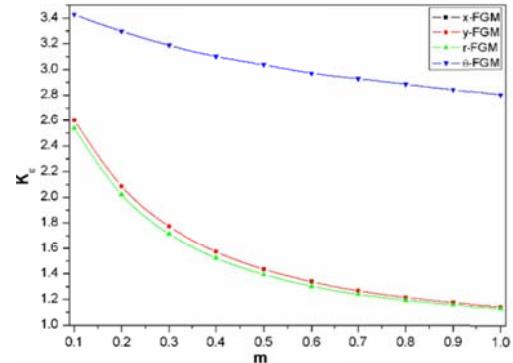


Fig. 13 Influence of m on K_{ϵ} under loading at cutout edge

the direction of material gradation and the other load is perpendicular to the same. Hence high stress zones are created in the material interfaces.

Fig. 11 shows the variation of K_{ϵ} at different m for biaxial case $\sigma_x = -\sigma_y$. It is seen that for all UDFGMs K_{ϵ} decreases as m increases. This is because as m increase the material distribution across the FGM plates approaches linearity and at $m=1$ it is exactly linear. This may be attributed to the fact that stress concentration will be always less if the material property changes gradually. This fact has been exploited by many designers while designing dissimilar metal welds using transition welding or laser engineered net shaping (LENS) (Carroll *et al.* 2015) (Durejko, Zi{k{e}}tala, Polkowski & Czujko 2014). Several cases of reducing stress around holes by proving FGM rings can also be found in literature (Sburlati R. 2013) (Yang, Gao, & Chen 2010) (Sburlati, Atashipour & Atashipour 2014).

4.3 In-plane loading at cut-out

Fig. 12 shows the variation of stress concentration factor with respect to material composition constant, m in a FGM plate loaded in in-plane direction at the cut-out. It is seen that K_{σ} trend lines in x-FGM and y-FGM are overlapping. This is because a square plate has been considered in this study, thus the variation in material properties in X-direction in x-FGM is ‘almost’ similar to variation of material properties in Y-direction in y-FGM (for the same m). The variation in material properties is referred here as being almost similar although theoretically the variation should have been exactly similar. This is because ANSYS does not contain any dedicated module to simulate FGM, thus, in the present work material properties are assigned to each element individually by using an APDL code. These lead to a discontinuous step-wise variation in properties. Also owing to the manual assignment of properties to each element, same material property at the boundary could not be ensured while comparing x-FGM to y-FGM. For instance, though theoretically the boundary values of materials have been assumed to be 107 GPa and 375 GPa, in the current simulation the Young’s modulus ranges from 107458 MPa–374810 MPa in x-FGM and between 107471 MPa – 374817 MPa in y-FGM.

From Fig. 12 it is also observed that K_{σ} is maximum in θ -FGM plates and least in r-FGM plates. From Fig. 4(c) it is seen that at the cutout boundary only one material (with highest E) is present and the material property radially changes. When the plate is loaded at the cutout boundary, the

vicinity of the cutout being much stiffer than the rest of the plate (again, due to being made of material with higher E) will undergo very small deformation. Thus for the r-FGM plates both K_σ and K_ε is least. In case of θ -FGM (Fig.4d) the material at the cutout boundary vary continuously, thus due to the presence of material variation at interfaces along the cutout boundary, localized stresses are produced. This leads to high K_σ . Also from Fig. 13 it is observed that K_ε is highest in θ -FGM plates.

5. Conclusions

For designing engineering structures with a circular cutout, a reliable estimation of SCFs is must. The paper successfully highlights the effect of material composition parameter in FGM plates. From the numerical simulations, the following inferences can be drawn,

- Material composition parameter (m) has a significant effect on stress and strain concentration factor.
- Maximum stress concentration K_σ will always occur when the FGM is loaded perpendicular to the direction of material gradation. Thus, K_σ is maximum in y-FGMs when FGMs are loaded uni-directionally in X-direction and for biaxially loaded FGMs maximum K_σ is seen in x-FGM and y-FGM.
- In general, K_ε decreases with increase in material composition parameter (m) for x-FGM, y-FGM and r-FGM.
- Strain concentration, K_ε is always more in θ -FGM as compared to other UDFGMs.

Acknowledgments

We thank Sayahnya Roy for his assistance with the artwork. We are also thankful to the anonymous referees for their valuable comments.

References

- Carroll, J., Adams, D.P., Maguire, M.C., Bishop, J.E., Reedlunn, B., Song, B., . . . others. (2015), "Variability in mechanical properties of laser engineered net shaping material. Tech. rep., Sandia national laboratories (SNL-NM), Albuquerque, NM (United States); Sandia National Laboratories, Livermore, CA.
- Dag, S., Ilhan, K. and Erdogan, F. (2008), "Mixed-mode stress intensity factors for an embedded crack in an orthotropic FGM coating", *Multiscale and functionally graded materials 2006:(M&FGM 2006)*, **973**, 16-21.
- Darwish, F., Gharaibeh, M. and Tashtoush, G. (2012), "A modified equation for the stress concentration factor in countersunk holes", *Eur. J. Mech.-A/Solids*, **36**, 94-103.
- Ding, S.H. and Li, X. (2008), "Anti-plane problem of periodic interface cracks in a functionally graded coating-substrate structure", *Int. J. Fract.*, **153**(1), 53-62.
- Durejko, T., Zi{\k{e}}tala, M., Polkowski, W. and Czujko, T. (2014), "Thin wall tubes with Fe 3 Al/SS316L graded structure obtained by using laser engineered net shaping technology", *Mater. Des.*, **63**, 766-774.
- Enab, T.A. (2012), "A comparative study of the performance of metallic and FGM tibia tray components in

- total knee replacement joints”, *Comput. Mater. Sci.*, **53**(1), 94-100.
- Enab, T.A. (2014), “Stress concentration analysis in functionally graded plates with elliptic holes under biaxial loadings”, *Ain Shams Eng. J.*, **5**(3), 839-850.
- Kalita, K. and Halder, S. (2014), “Static analysis of transversely loaded isotropic and orthotropic plates with central cutout”, *J. Inst. Eng. (India): Series C*, **95**(4), 347-358.
- Kalita, K., Shinde, D. and Thomas, T.T. (2015), “Non-dimensional stress analysis of an orthotropic plate”, *Mater. Today: Proc.*, **2**(4), 3527-3533.
- Kim, J.H. and Amit, K. (2008), “A generalized interaction integral method for the evaluation of the T-stress in orthotropic functionally graded materials under thermal loading”, *J. Appl. Mech.*, **75**(5), 051112.
- Kumar, A., Agrawal, A., Ghadai, R. and Kalita, K. (2016), “Analysis of stress concentration in orthotropic laminates”, *Procedia Tech.*, **23**, 156-162.
- Li, Y.D. and Lee, K.Y. (2008), “Fracture analysis of a weak-discontinuous interface in a symmetrical functionally gradient composite strip loaded by anti-plane impact”, *Arch. Appl. Mech.*, **78**(11), 855-866.
- Nemat-Alla, M. (2003), “Reduction of thermal stresses by developing two-dimensional functionally graded materials”, *Int. J. Solid. Struct.*, **40**(26), 7339-7356.
- Oonishi, H., Noda, T., Ito, S., Kohda, A., Ishimaru, H., Yamamoto, M. and Tsuji, E. (1994), “Effect of hydroxyapatite coating on bone growth into porous titanium alloy implants under loaded conditions”, *J. Appl. Biomater.*, **5**(1), 23-37.
- Saini, P.K. and Kushwaha, M. (2014), “Stress variation around a circular hole in functionally graded plate under bending”, *Int. J. Mech., Aerospace, Ind. Mechatronics Eng.*, **8**(3), 536-540.
- Sburlati, R. (2013), “Stress concentration factor due to a functionally graded ring around a hole in an isotropic plate”, *Int. J. Solid. Struct.*, **50**(22), 3649-3658.
- Sburlati, R., Atashipour, S.R. and Atashipour, S.A. (2014), “Reduction of the stress concentration factor in a homogeneous panel with hole by using a functionally graded layer”, *Compos. Part B: Eng.*, **61**, 99-109.
- Shao, Z., Ang, K., Reddy, J. and Wang, T. (2008), “Nonaxisymmetric thermomechanical analysis of functionally graded hollow cylinders”, *J. Therm. Stresses*, **31**(6), 515-536.
- Shen, H.S. and Noda, N. (2007), “Postbuckling of pressure-loaded FGM hybrid cylindrical shells in thermal environments”, *Compos. Struct.*, **77**(4), 546-560.
- Shokrolahi-Zadeh, B. and Shodja, H. (2008), “Spectral equivalent inclusion method: anisotropic cylindrical multi-inhomogeneities”, *J. Mech. Phys. Solids*, **56**(12), 3565-3575.
- Singh, B., Rokne, J. and Dhaliwal, R. (2008), “Vibrations of a solid sphere or shell of functionally graded materials”, *Eur. J. Mech.-A/Solids*, **27**(3), 460-468.
- Wang, B., Mai, Y.W. and Zhang, X. (2005), “Functionally graded materials under severe thermal environments”, *J. Am. Ceramic Soc.*, **88**(3), 683-690.
- Watari, F. (1997), “Elemental mapping of functionally graded dental implant in biocompatibility test”, *Functionally Graded Mater.*, **1996**, 749-754.
- Yamanouchi, M. and Koizumi, M. (1991), Functionally gradient materials.
- Yang, Q., Gao, C.F. and Chen, W. (2010), “Stress analysis of a functional graded material plate with a circular hole”, *Arch. Appl. Mech.*, **80**(8), 895-907.
- Yang, Z., Kim, C.B., Cho, C. and Beom, H.G. (2008), “The concentration of stress and strain in finite thickness elastic plate containing a circular hole”, *Int. J. Solid. Struct.*, **45**(3), 713-731.
- Young, W.C. and Budynas, R.G. (2002), *Roark's formulas for stress and strain* (Vol. 7), McGraw-Hill New York.
- Zhang, Z., Paulino, G.H. and Celes, W. (2008), “Cohesive modeling of dynamic crack growth in homogeneous and functionally graded materials”, *Multiscale Funct. Grad. Mater*, **973**, 562-567.
- Zhong, Z. and Cheng, Z. (2008), “Fracture analysis of a functionally graded strip with arbitrary distributed material properties”, *Int. J. Solid. Struct.*, **45**(13), 3711-3725.